Collision-System and Beam-Energy Dependence of Anisotropic Flow Fluctuations

M. S. Abdallah,[5] J. Adam,[6] L. Adamczyk,[2] J. R. Adams,[39] J. K. Adkins,[30] G. Agakishiev,[28] I. Aggarwal,[41] M. M. Aggarwal,[41] Z. Ahammed,[60] I. Alekseev,[3,35] D. M. Anderson,[55] A. Aparin,[28] E. C. Aschenauer,[6] M. U. Ashraf,[11] F. G. Atetalla,[29] A. Attri,[41] G. S. Averichev,[28] V. Bairathi,[53] W. Baker,[10] J. G. Ball Cap,[20] K. Barish,[10] A. Behera,[52] R. Bellwied,[20] P. Bhagat,[27] A. Bhasin,[27] J. Bielcik,[14] J. Bielcikova,[38] I. G. Bordyuzhin,[3] J. D. Brandenburg,[6] A. V. Brandin,[35] I. Bunzarov,[28] J. Butterworth,[45] X. Z. Cai,[50] H. Caines,[63] M. Calderón de la Barca Sánchez,[8] D. Cebra,[8] I. Chakaberia,[31,6] P. Chaloupka,[14] B. K. Chan,[9] F-H. Chang,[37] Z. Chang,[6] N. Chankova-Bunzarova,[28] A. Chatterjee,[11] S. Chattopadhyay,[60] D. Chen,[10] J. Chen,[49] J. H. Chen,[18] X. Chen,[48] Z. Chen,[49] J. Cheng,[57] M. Chevalier,[10] S. Choudhury,[18] W. Christie,[6] X. Chu,[6] H. J. Crawford,[7] M. Csanád,[16] M. Daugherity,[1] T. G. Dedovich,[28] I. M. Deppner,[19] A. A. Derevschikov,[43] A. Dhamija,[41] L. Di Carlo,[62] L. Didenko,[6] P. Dixit,[22] X. Dong,[31] J. L. Drachenberg,[1] E. Duckworth,[29] J. C. Dunlop,[6] N. Elsey,[62] J. Engelage,[7] G. Eppley,[45] S. Esumi,[58] O. Evdokimov,[12] A. Ewigleben,[32] O. Eyser,[6] R. Fatemi,[30] F. M. Fawzi,[5] S. Fazio,[6] P. Federic,[38] J. Fedorisin,[28] C. J. Feng,[37] Y. Feng,[44] P. Filip,[28] E. Finch,[51] Y. Fisyak,[6] A. Francisco,[63] C. Fu,[11] L. Fulek,[2] C. A. Gagliardi,[55] T. Galatyuk,[15] F. Geurts,[45] N. Ghimire,[54] A. Gibson,[59] K. Gopal,[23] X. Gou,[49] D. Grosnick,[59] A. Gupta,[27] W. Guryn,[6] A. I. Hamad,[29] A. Hamed,[5] Y. Han,[45] S. Harabasz,[15] M. D. Harasty,[8] J. W. Harris,[63] H. Harrison,[30] S. He,[11] W. He,[18] X. H. He,[26] Y. He,[49] S. Heppelmann,[8] S. Heppelmann,[42] N. Herrmann,[19] E. Hoffman,[20] L. Holub,[14] Y. Hu,[18] H. Huang,[37] H. Z. Huang,[9] S. L. Huang,[52] T. Huang,[37] X. Huang,[57] Y. Huang,[57] T. J. Humanic,[39] G. Igo,[9,*] D. Isenhower,[1] W. W. Jacobs,[25] C. Jena,[23] A. Jentsch,[6] Y. Ji,[31] J. Jia,[6,52] K. Jiang,[48] X. Ju,[48] E. G. Judd,[7] S. Kabana,[53] M. L. Kabir,[10] S. Kagamaster,[32] D. Kalinkin,[25,6] K. Kang,[57] D. Kapukchyan,[10] K. Kauder,[6] H. W. Ke,[6] D. Keane,[29] A. Kechechyan,[28] M. Kelsey,[62] Y. V. Khyzhniak,[35] D. P. Kikoła,[61] C. Kim,[10] B. Kimelman,[8] D. Kincses,[16] I. Kisel,[17] A. Kiselev,[6] A. G. Knospe,[32] L. Kochenda,[35] L. K. Kosarzewski,[14] L. Kramarik,[14] P. Kravtsov,[35] L. Kumar,[41] S. Kumar,[26] R. Kunnawalkam Elayavalli,[63] J. H. Kwasizur,[25] R. Lacey,[52] S. Lan,[11] J. M. Landgraf,[6] J. Lauret,[6] A. Lebedev,[6] R. Lednicky,[28,38] J. H. Lee,[6] Y. H. Leung,[31] C. Li,[49] C. Li,[48] W. Li,[45] X. Li,[48] Y. Li,[57] X. Liang,[10] Y. Liang,[29] R. Licenik,[38] T. Lin,[49] Y. Lin,[11] M. A. Lisa,[39] F. Liu,[11] H. Liu,[25] H. Liu,[11] P. Liu,[52] T. Liu,[63] X. Liu,[39] Y. Liu,[55] Z. Liu,[48] T. Ljubicic,[6] W. J. Llope,[62] R. S. Longacre,[6] E. Loyd,[10] N. S. Lukow,[54] X. F. Luo,[11] L. Ma,[18] R. Ma,[6] Y. G. Ma,[18] N. Magdy,[12] D. Mallick,[36] S. Margetis,[29] C. Markert,[56] H. S. Matis,[31] J. A. Mazer,[46] N. G. Minaev,[43] S. Mioduszewski,[55] B. Mohanty,[36] M. M. Mondal,[52] I. Mooney,[62] D. A. Morozov,[43] A. Mukherjee,[16] M. Nagy,[16] J. D. Nam,[54] Md. Nasim,[22] K. Nayak,[11] D. Neff,[9] J. M. Nelson,[7] D. B. Nemes,[63] M. Nie,[49] G. Nigmatkulov,[35] T. Niida,[58] R. Nishitani,[58] L. V. Nogach,[43] T. Nonaka,[58] A. S. Nunes,[6] G. Odyniec,[31] A. Ogawa,[6] S. Oh,[31] V. A. Okorokov,[35] B. S. Page,[6] R. Pak,[6] A. Pandav,[36] A. K. Pandey,[58] Y. Panebratsev,[28] P. Parfenov,[35] B. Pawlik,[40] D. Pawlowska,[61] H. Pei,[11] C. Perkins,[7] L. Pinsky,[20] R. L. Pintér,[16] J. Pluta,[61] B. R. Pokhrel,[54] G. Ponimatkin,[38] J. Porter,[31] M. Posik,[54] V. Prozorova,[14] N. K. Pruthi,[41] M. Przybycien,[2] J. Putschke,[62] H. Qiu,[26] A. Quintero,[54] C. Racz,[10] S. K. Radhakrishnan,[29] N. Raha,[62] R. L. Ray,[56] R. Reed,[32] H. G. Ritter,[31] M. Robotkova,[38] O. V. Rogachevskiy,[28] J. L. Romero,[8] D. Roy,[46] L. Ruan,[6] J. Rusnak,[38] N. R. Sahoo,[49] H. Sako,[58] S. Salur,[46] J. Sandweiss,[63,*] S. Sato,[58] W. B. Schmidke,[6] N. Schmitz,[33] B. R. Schweid,[52] F. Seck,[15] J. Seger,[13] M. Sergeeva,[9] R. Seto,[10] P. Seyboth,[33] N. Shah,[24] E. Shahaliev,[28] P. V. Shanmuganathan,[6] M. Shao,[48] T. Shao,[18] A. I. Sheikh,[29] D. Shen,[50] S. S. Shi,[11] Y. Shi,[49] Q. Y. Shou,[18] E. P. Sichtermann,[31] R. Sikora,[2] M. Simko,[38] J. Singh,[41] S. Singha,[26] M. J. Skoby,[44] N. Smirnov,[63] Y. Söhngen,[19] W. Solyst,[25] P. Sorensen,[6] H. M. Spinka,[4,*] B. Srivastava,[44] T. D. S. Stanislaus,[59] M. Stefaniak,[61] D. J. Stewart,[63] M. Strikhanov,[35] B. Stringfellow,[44] A. A. P. Suaide,[47] M. Sumbera,[38] B. Summa,[42] X. M. Sun,[11] X. Sun,[12] Y. Sun,[48] Y. Sun,[21] B. Surrow,[54] D. N. Svirida,[3] Z. W. Sweger,[8] P. Szymanski,[61] A. H. Tang,[6] Z. Tang,[48] A. Taranenko,[35] T. Tarnowsky,[34] J. H. Thomas,[31] A. R. Timmins,[20] D. Tlusty,[13] T. Todoroki,[58] M. Tokarev,[28] C. A. Tomkiel,[32] S. Trentalange,[9] R. E. Tribble,[55] P. Tribedy,[6] S. K. Tripathy,[16] T. Truhlar,[14] B. A. Trzeciak,[14] O. D. Tsai,[9] Z. Tu,[6] T. Ullrich,[6] D. G. Underwood,[4,59] I. Upsal,[49,6] G. Van Buren,[6] J. Vanek,[38] A. N. Vasiliev,[43] I. Vassiliev,[17] V. Verkest,[62] F. Videbæk,[6] S. Vokal,[28] S. A. Voloshin,[62] G. Wang,[9] J. S. Wang,[21] P. Wang,[48] Y. Wang,[11] Y. Wang,[57] Z. Wang,[49] J. C. Webb,[6] P. C. Weidenkaff,[19] L. Wen,[9] G. D. Westfall,[34] H. Wieman,[31] S. W. Wissink,[25] J. Wu,[26] Y. Wu,[10] B. Xi,[50] Z. G. Xiao,[57] G. Xie,[31] W. Xie,[44] H. Xu,[21] N. Xu,[31] Q. H. Xu,[49] Y. Xu,[49] Z. Xu,[6] Z. Xu,[9] C. Yang,[49] Q. Yang,[49] S. Yang,[45] Y. Yang,[37] Z. Ye,[45] Z. Ye,[12] L. Yi,[49] K. Yip,[6] Y. Yu,[49] H. Zbroszczyk,[61] W. Zha,[48] C. Zhang,[52] D. Zhang,[11] J. Zhang,[49] S. Zhang,[12] S. Zhang,[18] X. P. Zhang,[57] Y. Zhang,[26] Y. Zhang,[48] Y. Zhang,[11] Z. J. Zhang,[37] Z. Zhang,[6] Z. Zhang,[12] J. Zhao,[44] C. Zhou,[18] X. Zhu,[57] Z. Zhu,[49] M. Zurek,[4] and M. Zyzak[17]

(STAR Collaboration)

[1]*Abilene Christian University, Abilene, Texas 79699*
[2]*AGH University of Science and Technology, FPACS, Cracow 30-059, Poland*
[3]*Alikhanov Institute for Theoretical and Experimental Physics NRC "Kurchatov Institute," Moscow 117218*
[4]*Argonne National Laboratory, Argonne, Illinois 60439*
[5]*American University of Cairo, New Cairo 11835, New Cairo, Egypt*
[6]*Brookhaven National Laboratory, Upton, New York 11973*
[7]*University of California, Berkeley, California 94720*
[8]*University of California, Davis, California 95616*
[9]*University of California, Los Angeles, California 90095*
[10]*University of California, Riverside, California 92521*
[11]*Central China Normal University, Wuhan, Hubei 430079*
[12]*University of Illinois at Chicago, Chicago, Illinois 60607*
[13]*Creighton University, Omaha, Nebraska 68178*
[14]*Czech Technical University in Prague, FNSPE, Prague 115 19, Czech Republic*
[15]*Technische Universität Darmstadt, Darmstadt 64289, Germany*
[16]*ELTE Eötvös Loránd University, Budapest, Hungary H-1117*
[17]*Frankfurt Institute for Advanced Studies FIAS, Frankfurt 60438, Germany*
[18]*Fudan University, Shanghai, 200433*
[19]*University of Heidelberg, Heidelberg 69120, Germany*
[20]*University of Houston, Houston, Texas 77204*
[21]*Huzhou University, Huzhou, Zhejiang 313000*
[22]*Indian Institute of Science Education and Research (IISER), Berhampur 760010, India*
[23]*Indian Institute of Science Education and Research (IISER) Tirupati, Tirupati 517507, India*
[24]*Indian Institute Technology, Patna, Bihar 801106, India*
[25]*Indiana University, Bloomington, Indiana 47408*
[26]*Institute of Modern Physics, Chinese Academy of Sciences, Lanzhou, Gansu 730000*
[27]*University of Jammu, Jammu 180001, India*
[28]*Joint Institute for Nuclear Research, Dubna 141 980*
[29]*Kent State University, Kent, Ohio 44242*
[30]*University of Kentucky, Lexington, Kentucky 40506-0055*
[31]*Lawrence Berkeley National Laboratory, Berkeley, California 94720*
[32]*Lehigh University, Bethlehem, Pennsylvania 18015*
[33]*Max-Planck-Institut für Physik, Munich 80805, Germany*
[34]*Michigan State University, East Lansing, Michigan 48824*
[35]*National Research Nuclear University MEPhI, Moscow 115409*
[36]*National Institute of Science Education and Research, HBNI, Jatni 752050, India*
[37]*National Cheng Kung University, Tainan 70101*
[38]*Nuclear Physics Institute of the CAS, Rez 250 68, Czech Republic*
[39]*The Ohio State University, Columbus, Ohio 43210*
[40]*Institute of Nuclear Physics PAN, Cracow 31-342, Poland*
[41]*Panjab University, Chandigarh 160014, India*
[42]*Pennsylvania State University, University Park, Pennsylvania 16802*
[43]*NRC "Kurchatov Institute," Institute of High Energy Physics, Protvino 142281*
[44]*Purdue University, West Lafayette, Indiana 47907*
[45]*Rice University, Houston, Texas 77251*
[46]*Rutgers University, Piscataway, New Jersey 08854*
[47]*Universidade de São Paulo, São Paulo, Brazil 05314-970*
[48]*University of Science and Technology of China, Hefei, Anhui 230026*
[49]*Shandong University, Qingdao, Shandong 266237*
[50]*Shanghai Institute of Applied Physics, Chinese Academy of Sciences, Shanghai 201800*
[51]*Southern Connecticut State University, New Haven, Connecticut 06515*
[52]*State University of New York, Stony Brook, New York 11794*
[53]*Instituto de Alta Investigación, Universidad de Tarapacá, Arica 1000000, Chile*
[54]*Temple University, Philadelphia, Pennsylvania 19122*
[55]*Texas A&M University, College Station, Texas 77843*
[56]*University of Texas, Austin, Texas 78712*
[57]*Tsinghua University, Beijing 100084*
[58]*University of Tsukuba, Tsukuba, Ibaraki 305-8571, Japan*
[59]*Valparaiso University, Valparaiso, Indiana 46383*
[60]*Variable Energy Cyclotron Centre, Kolkata 700064, India*

[61]Warsaw University of Technology, Warsaw 00-661, Poland
[62]Wayne State University, Detroit, Michigan 48201
[63]Yale University, New Haven, Connecticut 06520

(Received 25 January 2022; revised 17 August 2022; accepted 16 November 2022; published 12 December 2022)

Elliptic flow measurements from two-, four-, and six-particle correlations are used to investigate flow fluctuations in collisions of U + U at $\sqrt{s_{\mathrm{NN}}} = 193$ GeV, Cu + Au at $\sqrt{s_{\mathrm{NN}}} = 200$ GeV and Au + Au spanning the range $\sqrt{s_{\mathrm{NN}}} = 11.5$–200 GeV. The measurements show a strong dependence of the flow fluctuations on collision centrality, a modest dependence on system size, and very little if any, dependence on particle species and beam energy. The results, when compared to similar LHC measurements, viscous hydrodynamic calculations, and TRENTO model eccentricities, indicate that initial-state-driven fluctuations predominate the flow fluctuations generated in the collisions studied.

DOI: 10.1103/PhysRevLett.129.252301

A wealth of studies of heavy-ion collisions at the Relativistic Heavy Ion Collider (RHIC) and the Large Hadron Collider (LHC) indicate that an exotic state of matter, called the Quark-Gluon Plasma (QGP), is created in the hot and dense environment present in these collisions. Ongoing studies at RHIC and the LHC are focused on developing a complete understanding of the dynamical evolution and the transport properties of the QGP.

Several analysis techniques have been employed to study the QGP. In particular, azimuthal anisotropy measurements of the produced particles have been used to study the viscous hydrodynamic response of the QGP to the spatial distribution of the initial energy density produced in the early stages of the collisions [1–12]. The azimuthal anisotropy of the particles produced relative to the flow planes Ψ_n, can be quantified via Fourier decomposition [13,14] of the distribution of their azimuthal angle (ϕ):

$$\frac{dN}{d\phi} \propto 1 + 2\sum_{n=1}^{\infty} v_n \cos[n(\phi - \Psi_n)], \qquad (1)$$

where the first Fourier harmonic v_1 is termed directed flow; v_2 is termed elliptic flow; v_3 is termed triangular flow, etc. A wealth of information on the characteristics of the QGP has been gained via studies of directed and elliptic flow [15–33], higher-order flow harmonics $v_{n>2}$ [8,24,34–43], flow fluctuations [44–54], the correlations between different flow harmonics [41,55–60], and correlations of symmetry planes [57,61–67].

Anisotropic flow driven by the spatial anisotropy of the initial-state energy density is characterized by the eccentricity vectors [49,68–71]:

$$\mathcal{E}_n \equiv \varepsilon_n e^{in\Phi_n} \equiv -\frac{\int d^2r_\perp r^n e^{in\varphi}\rho_e(r,\varphi)}{\int d^2r_\perp r^n \rho_e(r,\varphi)}, \qquad (n > 1), \quad (2)$$

where $\varepsilon_n = \langle|\mathcal{E}_n|^2\rangle^{1/2}$ and Φ_n are the magnitudes and azimuthal directions of the eccentricity vectors, φ is the spatial azimuthal angle, and $\rho_e(r,\varphi)$ represents the initial anisotropic energy density profile [65,71,72].

The v_2 and v_3 harmonics are, to a reasonable approximation, linearly related to the initial-state anisotropies, ε_2 and ε_3, respectively [6,49,73–79]:

$$v_n = \kappa_n \varepsilon_n, \qquad n = 2, 3, \qquad (3)$$

where κ_n encodes the medium response which is sensitive to the specific viscosity, i.e., the ratio of dynamic viscosity to entropy density η/s. Precision extractions of η/s require reliable model constraints for initial-state eccentricities and their fluctuations across a broad range of beam energies and collision systems [80,81]. Such constraints can be achieved via measurements of the flow harmonics and the event-by-event flow fluctuations for different systems and collision energies [49].

Flow fluctuations could arise from several underlying sources. They could develop in the initial state due to density fluctuations, during hydrodynamic evolution due to dissipation, and during hadronization. The precise role of the initial-state eccentricity fluctuations has attracted considerable recent attention [82–84]. However, the importance of the respective fluctuation sources has not been fully charted.

The multiparticle flow harmonics $v_n\{k\}$, with cumulants order $k = 2$, 4, and 6, obtained via multiparticle correlation methods [85,86] can give direct access to the event-by-event flow fluctuations [87,88]. Consequently, extensive measurements of $v_n\{k\}$ for different collision systems and beam energies could help to disentangle the fluctuation contributions from their respective sources, as well as establish whether flow fluctuations depend on the temperature, T, baryon chemical potential μ_B, or both. It could also provide unique supplemental constraints to distinguish between different initial-state models and reduce the fluctuations-related uncertainties associated with the extraction of $\eta/s(T, \mu_B)$.

In this Letter, we report new flow fluctuation measurements in collisions of U + U at $\sqrt{s_{\mathrm{NN}}} = 193$ GeV, Cu + Au at $\sqrt{s_{NN}} = 200$ GeV and Au + Au spanning the range $\sqrt{s_{NN}} = 11.5$–200 GeV. The measurements are derived from the flow harmonics $v_2\{k\}$, extracted via multiparticle cumulants for $k = 2$, 4, and 6. The extractions are comprehensive and benefit from consistent analysis across all systems and beam energies. Several of the extracted values for $v_2\{2\}$ and $v_2\{4\}$, used in the fluctuations measurements, are in good agreement with earlier charged hadron $v_2\{2\}$ and $v_2\{4\}$ measurements for U + U ($\sqrt{s_{NN}} = 193$ GeV [89]) and Au + Au collisions spanning the range $\sqrt{s_{NN}} =$ 11.5–200 GeV [90,91].

The data reported in this analysis were recorded with a minimum-bias trigger using the STAR detector [92], with the low-energy Au + Au data being collected as a part of the STAR Beam Energy Scan (BES-I) program. The collision vertices were reconstructed using tracks measured with charged-particle trajectories detected in the STAR Time Projection Chamber (TPC) in a 0.5 T magnetic field pointing along the beam direction (z axis) [93]. Events were selected to be within a radius $r < 2$ cm relative to the beam axis and within specific ranges of the center of the TPC in the direction along the beam axis v_z with the values ± 30 cm for U + U at $\sqrt{s_{NN}} = 193$ GeV, Cu + Au at $\sqrt{s_{NN}} = 200$ GeV, and Au + Au at $\sqrt{s_{NN}} = 200$ GeV, ± 40 cm at $\sqrt{s_{NN}} = 54.4$, 39, 27, 19.6 GeV and ± 50 cm at $\sqrt{s_{NN}} = 11.5$ GeV.

The collision centrality was determined via a Monte Carlo Glauber calculation tuned to match the event-by-event multiplicity measurements [90,94]. Analyzed tracks were required to have a distance of closest approach (DCA) to the primary vertex of < 3 cm, and to have more than 15 out of a possible 45 TPC space points used in their reconstruction. Furthermore, the ratio of the number of fit points used to the maximum possible number of TPC space points was required to be larger than 0.52 to remove split tracks. The transverse momentum (p_T) of the tracks was limited to $0.2 < p_T < 4.0$ GeV/c for charged particles and to $0.2 < p_T < 2.0$ GeV/c for the identified particle species. Particle identification (for pi, K, p) is based on the compound use of the ionization energy loss, dE/dx, in the TPC [95], and the squared mass from the TOF [96] detector.

The operational framework of the multiparticle cumulant technique is given in Refs. [85,97] and its extension to the method of subevent cumulants is summarized in Ref. [86]. Particle pairs, quadruplets, and sextuplets were selected in the range $|\eta| < 1$. The $2m$-particle azimuthal correlator is obtained by averaging over all unique combinations in one event, then over all events [98]:

$$\langle\langle 2m \rangle\rangle = \langle\langle e^{in\sum_{j=1}^{m}(\phi_{2j-1}-\phi_{2j})} \rangle\rangle, \tag{4}$$

to give the four- and six-particle cumulants as

$$c_n\{4\} = \langle\langle 4 \rangle\rangle - 2\langle\langle 2 \rangle\rangle^2, \tag{5}$$

$$c_n\{6\} = \langle\langle 6 \rangle\rangle - 9\langle\langle 4 \rangle\rangle\langle\langle 2 \rangle\rangle + 12\langle\langle 2 \rangle\rangle^3. \tag{6}$$

The nonflow contributions to the two-particle cumulants, that typically involve particles emitted within a localized region in η, can be mitigated via the two-subevents method [86,99,100]. The associated two-particle cumulants can be expressed as

$$\langle\langle 2 \rangle\rangle_{a|b} = \langle\langle e^{in(\phi_1^a - \phi_2^b)} \rangle\rangle, \tag{7}$$

$$c_n\{2\} = \langle\langle 2 \rangle\rangle_{a|b}, \tag{8}$$

where Eqs. (5)–(8) lead to the following cumulant-based definitions for the two-, four-, and six-particle harmonic flow coefficients v_n:

$$v_n\{2\} = \sqrt{c_n\{2\}}, \tag{9}$$

$$v_n\{4\} = \sqrt[4]{-c_n\{4\}}, \tag{10}$$

$$v_n\{6\} = \sqrt[6]{c_n\{6\}/4}. \tag{11}$$

The subevents method was used to evaluate the two-particle cumulants for the nonoverlapping η interval $|\Delta\eta| > 0.6$ (*i.e.* $\eta^a > 0.3$ for subevent a and $\eta^b < -0.3$ for subevent b), but not the four- and six-particle cumulants due to the limited acceptance and statistics of the measurements. Instead, "traditional" four- and six-particle cumulants were obtained via the method with particle weights that reflect the efficiency and acceptance correction [85,97].

For a Gaussian distribution of the flow fluctuations, the fluctuations contributions to the nth-order flow harmonics can be written as [101,102]:

$$v_n\{2\} \approx \langle v_n \rangle + \sigma_n^2/(2\langle v_n \rangle), \tag{12}$$

$$v_n\{4\} \approx \langle v_n \rangle - \sigma_n^2/(2\langle v_n \rangle), \tag{13}$$

$$v_n\{6\} \approx \langle v_n \rangle - \sigma_n^2/(2\langle v_n \rangle). \tag{14}$$

Equations (12)–(14) are also valid for other distributions in the limit that the variance $\sigma_n \ll \langle v_n \rangle$. In this Letter, the ratio between the four-particle elliptic flow $v_2\{4\}$, and the two-particle nonflow-suppressed elliptic flow $v_2\{2\}$ at a given centrality, is used to estimate the strength of the elliptic flow fluctuations' relative to the measured elliptic flow strength [81,103]. Note that $v_2\{4\}/v_2\{2\} \approx 1.0$ indicates minimal, if any, fluctuations whereas $v_2\{4\}/v_2\{2\} < 1.0$ indicates more significant fluctuations as this ratio decreases.

The presented measurements' systematic uncertainties are obtained from variations in the analysis cuts for event selection, track selection, and nonflow suppression;

(i) event selection was varied via cuts on the vertex positions determined in the TPC along the beam direction v_z to $v_z > 0$ cm and $v_z < 0$ cm. (ii) Track selection was varied by (a) reducing the DCA from its nominal value of 3 to 2 cm, and (b) increasing the number of TPC space points used from more than 15 points to more than 20 points. (iii) The pseudorapidity gap, $\Delta\eta = \eta_1 - \eta_2$ for the track pairs, used to mitigate the nonflow effects due to resonance decays, Bose-Einstein correlations, and the fragments of individual jets, was varied from $|\Delta\eta| > 0.6$ to $|\Delta\eta| > 0.8$.

The $\Delta\eta$ cut does not entirely suppress possible long-range nonflow contributions (e.g., jets in a dijet event), which increase from central to peripheral events and decrease with beam energy. Estimates of the systematic uncertainty due to this residual nonflow contribution can be made via several techniques [104–107]. The peripheral subtraction method [104], which assumes that the long-range nonflow is independent of centrality, indicates uncertainties that range from 1% in central collisions to 13% in peripheral collisions at $\sqrt{s_{NN}} = 200$ GeV, and are included in the overall uncertainties. Because of the lower jet yields for beam energies $\lesssim$63 GeV [108], the much smaller associated uncertainties are not included in their respective overall systematic uncertainty estimate.

For identified particle species, the particle identification cuts were also varied about their nominal values [109]. The overall systematic uncertainty for identified and inclusive charged hadrons, assuming independent sources, was estimated via a quadrature sum of the uncertainties resulting from the respective cut variations. They range from 4% to 15% for $v_2\{2\}$, 2% to 4% for $v_2\{4\}$ and $v_2\{6\}$, and 4% to 13% for $v_2\{4\}/v_2\{2\}$, from central to peripheral collisions, depending on the beam energy. The nonflow-associated uncertainty dominates the overall uncertainty of $v_2\{4\}/v_2\{2\}$ since the effects of the other cut variations approximately cancel.

In Fig. 1 the p_T-integrated two-, four-, and six-particle elliptic flow (a) and the ratio $v_2\{4\}/v_2\{2\}$ (b), are presented as a function of centrality for Au + Au collisions at $\sqrt{s_{NN}} = 200$ GeV. Note that the range 1%–5% is used instead of 0%–5% [110] to ensure positive values for $v_2\{4\}$ in central collisions. Further study [88] is required to understand this sign change fully. Figure 1(a) shows the known characteristic centrality dependence of two-, four-, and six-particle elliptic flow, as well as quantitative agreement between $v_2\{4\}$ and $v_2\{6\}$. The difference between the magnitudes for $v_2\{2\}$ and those for $v_2\{4\}$ and $v_2\{6\}$ reflects the important role of the flow fluctuations. The similarity between $v_2\{4\}$ and $v_2\{6\}$, within statistical uncertainties, is consistent with a Gaussian hypothesis of the flow fluctuations. The ratio $v_2\{4\}/v_2\{2\}$, presented in Fig. 1(b), serves as a metric for elliptic flow fluctuations; it shows the expected decrease in the magnitude of the fluctuations from central to midcentral collisions, reminiscent of the pattern observed for the initial-state eccentricity

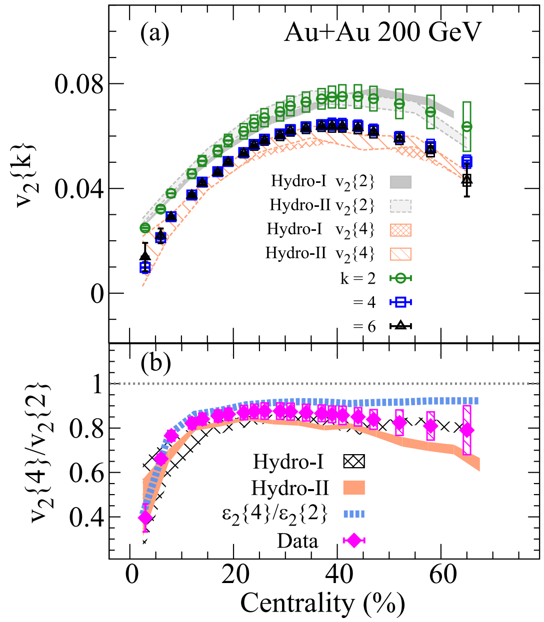

FIG. 1. Comparison of the charged hadrons two-, four-, and six-particle elliptic flow, $v_2\{k\}$, $k = 2$, 4, and 6, panel (a), and the ratio, $v_2\{4\}/v_2\{2\}$, panel (b), vs centrality, in the p_T range $0.2 - 4.0$ GeV/c for Au + Au collisions at $\sqrt{s_{NN}} = 200$ GeV; the range 1%–5% is used instead of 0%–5% [110] (see text). The vertical lines and the open boxes indicate the respective statistical and systematic uncertainties. The hatched bands and dashed curves represent the model calculations presented in Refs. [80] (Hydro-I) and [81] (Hydro-II), and the eccentricity ratio $\varepsilon_2\{4\}/\varepsilon_2\{2\}$ [81], as indicated.

fluctuations, $\varepsilon_2\{4\}/\varepsilon_2\{2\}$ [81], shown by the blue dashed curve. The hashed bands in Fig. 1 represent the results from two hydrodynamical model calculations [81,111]. Hydro-I [80,112] uses an IP-Glasma [113] inspired initial-state in conjunction with the UrQMD [114,115] afterburner. It also imposes the effects of global momentum conservation and the local charge conservation. Hydro-II [81] employs the TRENTO model [116] initial state and does not include the UrQMD afterburner. Both models show good qualitative agreement with the v_2 data [Fig. 1(a)]. The data-model comparisons in Fig. 1(b) indicate that Hydro-II [81] overpredicts the measurements in midcentral and peripheral collisions, but Hydro-I [80] is in good overall agreement with the presented measurements. The hydrodynamic model predictions contrast with the corresponding eccentricity fluctuations (dashed blue line) which appear to underpredict the measured fluctuations in peripheral events. The latter is to be expected if eccentricity fluctuations are not the only source of the flow fluctuations. However, possible residual nonflow contribution to $v_2\{2\}$ could also contribute to this difference. Nonetheless, the similarity between the centrality dependence of the ratio $\varepsilon_2\{4\}/\varepsilon_2\{2\}$, and that for the $v_2\{4\}/v_2\{2\}$ measurements, suggests that eccentricity fluctuations dominate the flow fluctuations in central and midcentral collisions.

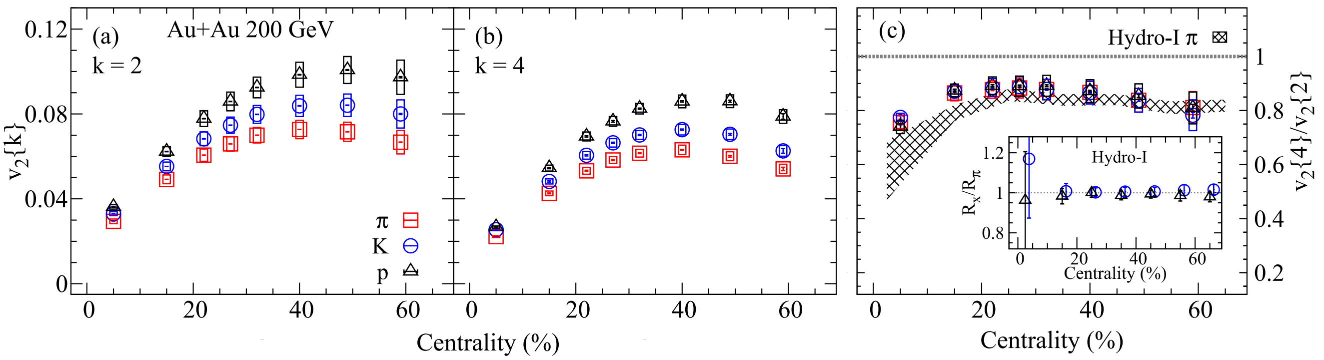

FIG. 2. Comparison of the centrality dependence of $v_2\{2\}$ (a), $v_2\{4\}$ (b), and the ratio $v_2\{4\}/v_2\{2\}$ (c), for different particle species in the p_T range $0.2-2.0$ GeV/c for Au + Au collisions at $\sqrt{s_{NN}} = 200$ GeV. The vertical lines and the open boxes indicate the respective statistical and systematic uncertainties. The hashed band in (c) shows the results for charged pions from Ref. [80] (Hydro-I). The inset shows the ratio $R_{K,p}/R_\pi$ ($R = v_2\{4\}/v_2\{2\}$) for the respective particle species.

The species dependence of the flow fluctuations can give insight on possible contributions from other fluctuation sources [83,117,118]. Here, an essential point is that the fluctuations generated during the hadronization of the QGP could lead to a difference in the magnitude of the fluctuations for different particle species. Figure 2 shows a comparison of the measured centrality dependence of $v_2\{2\}$ (a), $v_2\{4\}$ (b), and the ratio $v_2\{4\}/v_2\{2\}$ (c), for pions, kaons, and protons in Au + Au collisions at $\sqrt{s_{NN}} = 200$ GeV; for these $v_2\{4\}$ results, a procedure which uses one identified hadron and three inclusive charged hadrons was employed. The $v_2\{2\}$ and $v_2\{4\}$ measurements exhibit the well known mass ordering [119] for these particle species.

Figure 2(c) compares the $v_2\{4\}/v_2\{2\}$ ratios for pions, kaons, and protons; they indicate that the magnitude and trend of the flow fluctuations are independent of the particle species. The effects of mass ordering, apparent in Figs. 2(a) and 2(b), are expected to cancel in these ratios [81,83], but the fluctuations might not. Strikingly similar species independent patterns can also be seen for the ratios obtained from the Hydro-I calculations [111], shown by the hatched band and the inset in Fig. 2(c). A similar species independent result is obtained for Hydro-II [81], albeit with different magnitudes for the $v_2\{4\}/v_2\{2\}$ ratios. A species independent $v_2\{4\}/v_2\{2\}$ ratio is expected if initial-state fluctuations dominate over other sources of fluctuations.

The beam-energy dependence of the flow fluctuations can give insight into possible fluctuation sources associated with the expansion dynamics. Consequently, the flow and flow-fluctuation measurements were performed for Au + Au collisions spanning the range $\sqrt{s_{NN}} = 11.5$–200 GeV. Figure 3 gives a summary of the centrality dependence of $v_2\{2\}$ (a), $v_2\{4\}$ (b), $v_2\{6\}$ (c) and the ratios $v_2\{4\}/v_2\{2\}$ (d) and $v_2\{6\}/v_2\{4\}$ (e) for the respective beam energies indicated. Figures 3(a)–3(c) show an increase with increasing beam energy for the values of $v_2\{2\}$, $v_2\{4\}$, and $v_2\{6\}$, that reflects the change in the expansion dynamics.

The $v_2\{4\}/v_2\{2\}$ ratios shown in Fig. 3(d) suggest that within the given uncertainties, the flow fluctuations are weakly dependent on the beam energy, if at all, irrespective of the collision centrality. The magnitude and trend of these ratios are also comparable to those for the LHC measurements for Pb + Pb collisions at $\sqrt{s_{NN}} = 2.76$ TeV [120]

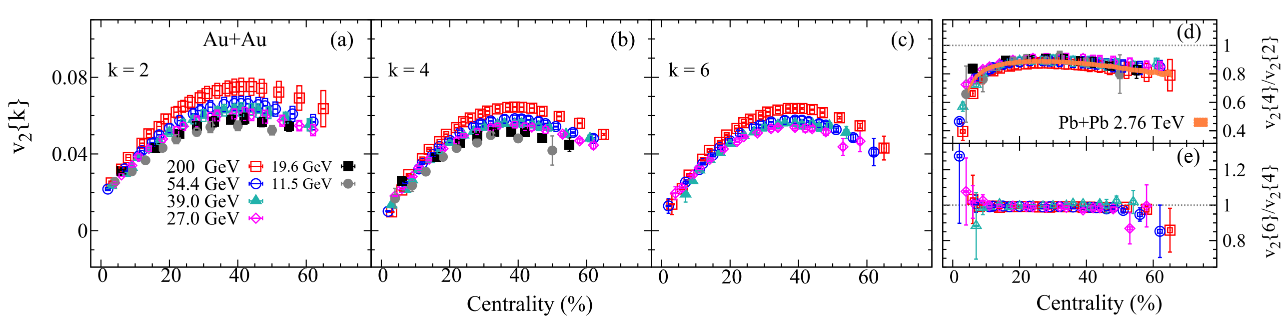

FIG. 3. Comparison of the centrality dependence of the charged hadrons $v_2\{2\}$ (a), $v_2\{4\}$ (b), $v_2\{6\}$ (c), and the ratios $v_2\{4\}/v_2\{2\}$ (d) and $v_2\{6\}/v_2\{4\}$ (e), in the p_T range $0.2-4.0$ GeV/c for Au + Au collisions at $\sqrt{s_{NN}} = 11.5$–200 GeV. The vertical lines and the open boxes indicate the respective statistical and systematic uncertainties. The shaded band in (d) indicates the ratios obtained from the LHC measurements for the p_T range $0.2-3.0$ GeV/c for Pb + Pb collisions at $\sqrt{s_{NN}} = 2.76$ TeV [120]; only statistical uncertainties are shown for the latter.

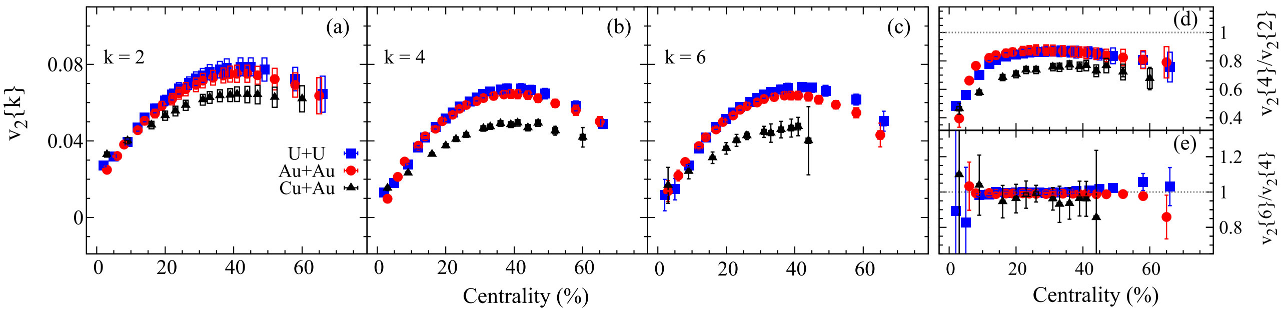

FIG. 4. Comparison of the centrality dependence of the charged hadrons $v_2\{2\}$ (a), $v_2\{4\}$ (b), $v_2\{6\}$ (c), and the ratios $v_2\{4\}/v_2\{2\}$ (d) and $v_2\{6\}/v_2\{4\}$ (e), in the p_T range $0.2-4.0$ GeV/c for U + U ($\sqrt{s_{NN}} = 193$ GeV), Au + Au and Cu + Au collisions at $\sqrt{s_{NN}} = 200$ GeV. The vertical lines and the open boxes indicate the respective statistical and systematic uncertainties.

and to the $\varepsilon_2\{4\}/\varepsilon_2\{2\}$ ratios, in central to midcentral collisions, shown in Fig. 1(b). They suggest that the flow fluctuations associated with the expansion dynamics do not change substantially over the beam energy range $\sqrt{s_{NN}} =$ 11.5–2760 GeV. The comparable magnitudes for $v_2\{4\}/v_2\{2\}$ and $\varepsilon_2\{4\}/\varepsilon_2\{2\}$ also suggest that the initial-state eccentricity fluctuations dominate the flow fluctuations encoded in the ratio $v_2\{4\}/v_2\{2\}$. The $v_2\{6\}/v_2\{4\}$ ratios in Fig. 3(e) indicate values which are systematically less than one, but with little if any, dependence on centrality. The latter pattern, which contrasts with similar LHC measurements [50–52], could be a further indication for the Gaussian-like nature of the flow fluctuations across the presented beam energies.

Further knowledge on the fluctuation sources can be obtained by comparing the measurements for collisions of U + U, Au + Au, and Cu + Au at similar collision energy. Here, it is noteworthy that the prolate deformation of uranium, the oblate deformation of Au, and the asymmetry and system size for Cu + Au collisions, can lead to different initial-state eccentricities for the same centrality, especially in central collisions. Figure 4 shows a summary of the centrality dependence of $v_2\{2\}$ (a), $v_2\{4\}$ (b), $v_2\{6\}$ (c) and the ratios $v_2\{4\}/v_2\{2\}$ (d) and $v_2\{6\}/v_2\{4\}$ (e) for U + U ($\sqrt{s_{NN}} = 193$ GeV), Au + Au and Cu + Au collisions at $\sqrt{s_{NN}} = 200$ GeV. Figures 4(a)–4(c) provide a clear indication that $v_2\{2\}$, $v_2\{4\}$, and $v_2\{6\}$ are system dependent and follows a system-size hierarchy with more pronounced differences for Cu + Au. This system-size hierarchy can be attributed to the system-dependent eccentricity hierarchy [121].

The $v_2\{4\}/v_2\{2\}$ ratios shown in Fig. 4(d), indicate the expected decrease in the magnitude of the fluctuations from central to peripheral collisions for all three systems. However, in contrast to the energy dependence shown in Fig. 3(d), the system dependence of the flow fluctuations is now apparent, albeit with a much smaller difference between U + U and Au + Au than the difference between Cu + Au and U + U or Au + Au. These results point to an increasingly important role for flow fluctuations as the system size is reduced. The magnitude and trends of the $v_2\{6\}/v_2\{4\}$ ratios in Fig. 4(e) are similar to those in Fig. 3(e), suggesting that the Gaussian-like nature of the flow fluctuations is system independent.

In summary, we have used the two- and multiparticle cumulants method to make comprehensive measurements of two-, four-, and six-particle elliptic flow and flow fluctuations in collisions of U + U at $\sqrt{s_{NN}} = 193$ GeV, Cu + Au at $\sqrt{s_{NN}} = 200$ GeV and Au + Au for the range $\sqrt{s_{NN}} = 11.5$–200 GeV. The measurements show the expected characteristic dependence of $v_2\{2\}$, $v_2\{4\}$, and $v_2\{6\}$ on centrality, system size, and beam energy. The elliptic-flow fluctuations extracted from these measurements indicate more substantial fluctuations in more central collisions, a dependence on collision system, and little if any dependence on particle species and beam energy. Comparisons of these results to similar LHC measurements, as well as to viscous hydrodynamical calculations and TRENTO model eccentricity ratios, suggest that initial-state-driven fluctuations dominate the flow fluctuations in the collisions studied. A complete set of model comparisons to this comprehensive data set is needed to flesh out the detailed initial- and final-state-driven contributions to flow fluctuations. The mapping of such contributions could serve to discern between different initial-state models, as well as constrain the fluctuations-related uncertainties associated with the extraction of $\eta/s(T, \mu_B)$.

We thank the RHIC Operations Group and RCF at BNL, the NERSC Center at LBNL, and the Open Science Grid consortium for providing resources and support. This work was supported in part by the Office of Nuclear Physics within the U.S. DOE Office of Science, the U.S. National Science Foundation, National Natural Science Foundation of China, Chinese Academy of Science, the Ministry of Science and Technology of China and the Chinese Ministry of Education, the Higher Education Sprout Project by Ministry of Education at NCKU, the National Research Foundation of Korea, Czech Science Foundation and Ministry of Education, Youth and Sports of the Czech Republic, Hungarian National Research, Development and

Innovation Office, New National Excellency Programme of the Hungarian Ministry of Human Capacities, Department of Atomic Energy and Department of Science and Technology of the Government of India, the National Science Centre and WUT ID-UB of Poland, the Ministry of Science, Education and Sports of the Republic of Croatia, German Bundesministerium für Bildung, Wissenschaft, Forschung and Technologie (BMBF), Helmholtz Association, Ministry of Education, Culture, Sports, Science, and Technology (MEXT) and Japan Society for the Promotion of Science (JSPS).

*Deceased.

[1] T. Hirano, U. W. Heinz, D. Kharzeev, R. Lacey, and Y. Nara, Phys. Lett. B **636**, 299 (2006).
[2] P. Huovinen, P. F. Kolb, U. W. Heinz, P. V. Ruuskanen, and S. A. Voloshin, Phys. Lett. B **503**, 58 (2001).
[3] T. Hirano and K. Tsuda, Phys. Rev. C **66**, 054905 (2002).
[4] P. Romatschke and U. Romatschke, Phys. Rev. Lett. **99**, 172301 (2007).
[5] M. Luzum, J. Phys. G **38**, 124026 (2011).
[6] H. Song, S. A. Bass, U. Heinz, T. Hirano, and C. Shen, Phys. Rev. Lett. **106**, 192301 (2011); **109**, 139904(E) (2012).
[7] J. Qian, U. W. Heinz, and J. Liu, Phys. Rev. C **93**, 064901 (2016).
[8] N. Magdy (STAR Collaboration), J. Phys. Conf. Ser. **779**, 012060 (2017).
[9] B. Schenke, S. Jeon, and C. Gale, Phys. Lett. B **702**, 59 (2011).
[10] D. Teaney and L. Yan, Phys. Rev. C **86**, 044908 (2012).
[11] F. G. Gardim, F. Grassi, M. Luzum, and J.-Y. Ollitrault, Phys. Rev. Lett. **109**, 202302 (2012).
[12] R. A. Lacey, D. Reynolds, A. Taranenko, N. N. Ajitanand, J. M. Alexander, F.-H. Liu, Y. Gu, and A. Mwai, J. Phys. G **43**, 10LT01 (2016).
[13] S. Voloshin and Y. Zhang, Z. Phys. C **70**, 665 (1996).
[14] A. M. Poskanzer and S. A. Voloshin, Phys. Rev. C **58**, 1671 (1998).
[15] B. Alver *et al.* (PHOBOS Collaboration), Phys. Rev. Lett. **98**, 242302 (2007).
[16] B. B. Back *et al.* (PHOBOS Collaboration), Phys. Rev. Lett. **97**, 012301 (2006).
[17] C. Adler *et al.* (STAR Collaboration), Phys. Rev. C **66**, 034904 (2002).
[18] J. Adams *et al.* (STAR Collaboration), Phys. Rev. Lett. **92**, 062301 (2004); **127**, 069901(E) (2021).
[19] K. H. Ackermann *et al.* (STAR Collaboration), Phys. Rev. Lett. **86**, 402 (2001).
[20] A. Adare *et al.* (PHENIX Collaboration), Phys. Rev. C **99**, 054903 (2019).
[21] K. Adcox *et al.* (PHENIX Collaboration), Phys. Rev. Lett. **89**, 212301 (2002).
[22] J. Adam *et al.* (STAR Collaboration), Phys. Rev. Lett. **122**, 172301 (2019).
[23] N. Magdy (STAR Collaboration), Nucl. Phys. **A982**, 255 (2019).
[24] K. Aamodt *et al.* (ALICE Collaboration), Phys. Rev. Lett. **107**, 032301 (2011).
[25] B. Abelev *et al.* (ALICE Collaboration), Phys. Lett. B **719**, 18 (2013).
[26] J. Adam *et al.* (ALICE Collaboration), Phys. Rev. Lett. **116**, 132302 (2016).
[27] J. Adam *et al.* (ALICE Collaboration), Phys. Lett. B **762**, 376 (2016).
[28] M. Aaboud *et al.* (ATLAS Collaboration), Eur. Phys. J. C **78**, 997 (2018).
[29] S. Chatrchyan *et al.* (CMS Collaboration), Phys. Rev. Lett. **109**, 022301 (2012).
[30] S. Chatrchyan *et al.* (CMS Collaboration), Phys. Rev. C **87**, 014902 (2013).
[31] S. Chatrchyan *et al.* (CMS Collaboration), Phys. Lett. B **724**, 213 (2013).
[32] S. Chatrchyan *et al.* (CMS Collaboration), Phys. Rev. C **89**, 044906 (2014).
[33] K. Aamodt *et al.* (ALICE Collaboration), Phys. Rev. Lett. **105**, 252302 (2010).
[34] B. Alver and G. Roland, Phys. Rev. C **81**, 054905 (2010); **82**, 039903(E) (2010).
[35] A. Adare *et al.* (PHENIX Collaboration), Phys. Rev. Lett. **107**, 252301 (2011).
[36] A. Adare *et al.* (PHENIX Collaboration), Phys. Rev. C **93**, 051902 (2016).
[37] G. Aad *et al.* (ATLAS Collaboration), Phys. Rev. C **92**, 034903 (2015).
[38] M. Aaboud *et al.* (ATLAS Collaboration), Eur. Phys. J. C **77**, 428 (2017).
[39] A. Adare *et al.* (PHENIX Collaboration), Phys. Rev. Lett. **107**, 252301 (2011).
[40] L. Adamczyk *et al.* (STAR Collaboration), Phys. Rev. C **98**, 014915 (2018).
[41] L. Adamczyk *et al.* (STAR Collaboration), Phys. Rev. C **98**, 034918 (2018).
[42] S. Chatrchyan *et al.* (CMS Collaboration), Phys. Rev. C **89**, 044906 (2014).
[43] A. M. Sirunyan *et al.* (CMS Collaboration), Phys. Rev. C **100**, 044902 (2019).
[44] B. Alver *et al.* (PHOBOS Collaboration), Phys. Rev. C **81**, 034915 (2010).
[45] B. Alver *et al.* (PHOBOS Collaboration), Phys. Rev. Lett. **104**, 142301 (2010).
[46] B. Alver *et al.* (PHOBOS Collaboration), Phys. Rev. C **77**, 014906 (2008).
[47] J.-Y. Ollitrault, A. M. Poskanzer, and S. A. Voloshin, Phys. Rev. C **80**, 014904 (2009).
[48] B. Alver *et al.* (PHOBOS Collaboration), Phys. Rev. C **81**, 034915 (2010).
[49] Z. Qiu and U. W. Heinz, Phys. Rev. C **84**, 024911 (2011).
[50] G. Aad *et al.* (ATLAS Collaboration), Eur. Phys. J. C **74**, 3157 (2014).
[51] A. M. Sirunyan *et al.* (CMS Collaboration), Phys. Lett. B **789**, 643 (2019).
[52] S. Acharya *et al.* (ALICE Collaboration), J. High Energy Phys. 07 (2018) 103.

[53] A. Adare *et al.* (PHENIX Collaboration), Phys. Rev. C **99**, 024903 (2019).
[54] M. Aaboud *et al.* (ATLAS Collaboration), J. High Energy Phys. 01 (2020) 051.
[55] G. Aad *et al.* (ATLAS Collaboration), Phys. Rev. C **92**, 034903 (2015).
[56] J. Adam *et al.* (STAR Collaboration), Phys. Lett. B **783**, 459 (2018).
[57] J. Adam *et al.* (STAR Collaboration), Phys. Lett. B **809**, 135728 (2020).
[58] S. Acharya *et al.* (ALICE Collaboration), Phys. Rev. Lett. **127**, 092302 (2021).
[59] S. Acharya *et al.* (ALICE Collaboration), Phys. Lett. B **818**, 136354 (2021).
[60] M. Aaboud *et al.* (ATLAS Collaboration), Phys. Lett. B **789**, 444 (2019).
[61] S. Acharya *et al.* (ALICE Collaboration), Phys. Lett. B **773**, 68 (2017).
[62] A. M. Sirunyan *et al.* (CMS Collaboration), Eur. Phys. J. C **80**, 534 (2020).
[63] N. Magdy, arXiv:2210.14091.
[64] N. Magdy, Phys. Rev. C **106**, 044911 (2022).
[65] L. Yan and J.-Y. Ollitrault, Phys. Lett. B **744**, 82 (2015).
[66] N. Magdy, J. Phys. G **49**, 015105 (2022).
[67] M. Aaboud *et al.* (ATLAS Collaboration), Eur. Phys. J. C **78**, 142 (2018).
[68] B. H. Alver, C. Gombeaud, M. Luzum, and J.-Y. Ollitrault, Phys. Rev. C **82**, 034913 (2010).
[69] H. Petersen, G.-Y. Qin, S. A. Bass, and B. Muller, Phys. Rev. C **82**, 041901(R) (2010).
[70] R. A. Lacey, R. Wei, J. Jia, N. N. Ajitanand, J. M. Alexander, and A. Taranenko, Phys. Rev. C **83**, 044902 (2011).
[71] D. Teaney and L. Yan, Phys. Rev. C **83**, 064904 (2011).
[72] R. S. Bhalerao, J.-Y. Ollitrault, and S. Pal, Phys. Lett. B **742**, 94 (2015).
[73] H. Niemi, G. S. Denicol, H. Holopainen, and P. Huovinen, Phys. Rev. C **87**, 054901 (2013).
[74] F. G. Gardim, J. Noronha-Hostler, M. Luzum, and F. Grassi, Phys. Rev. C **91**, 034902 (2015).
[75] J. Fu, Phys. Rev. C **92**, 024904 (2015).
[76] H. Holopainen, H. Niemi, and K. J. Eskola, Phys. Rev. C **83**, 034901 (2011).
[77] G.-Y. Qin, H. Petersen, S. A. Bass, and B. Muller, Phys. Rev. C **82**, 064903 (2010).
[78] C. Gale, S. Jeon, B. Schenke, P. Tribedy, and R. Venugopalan, Phys. Rev. Lett. **110**, 012302 (2013).
[79] P. Liu and R. A. Lacey, Phys. Rev. C **98**, 021902(R) (2018).
[80] B. Schenke, C. Shen, and P. Tribedy, Phys. Rev. C **99**, 044908 (2019).
[81] P. Alba, V. Mantovani Sarti, J. Noronha, J. Noronha-Hostler, P. Parotto, I. Portillo Vazquez, and C. Ratti, Phys. Rev. C **98**, 034909 (2018).
[82] S. Manly (PHOBOS Collaboration), Nucl. Phys. **A774**, 523 (2006).
[83] N. Magdy, X. Sun, Z. Ye, O. Evdokimov, and R. Lacey, Universe **6**, 146 (2020).
[84] S. Rao, M. Sievert, and J. Noronha-Hostler, Phys. Rev. C **103**, 034910 (2021).
[85] A. Bilandzic, C. H. Christensen, K. Gulbrandsen, A. Hansen, and Y. Zhou, Phys. Rev. C **89**, 064904 (2014).
[86] J. Jia, M. Zhou, and A. Trzupek, Phys. Rev. C **96**, 034906 (2017).
[87] N. Borghini, P. M. Dinh, and J.-Y. Ollitrault, Phys. Rev. C **63**, 054906 (2001).
[88] M. Aaboud *et al.* (ATLAS Collaboration), J. High Energy Phys. 1 (2020) 51.
[89] L. Adamczyk *et al.* (STAR Collaboration), Phys. Rev. Lett. **115**, 222301 (2015).
[90] L. Adamczyk *et al.* (STAR Collaboration), Phys. Rev. C **86**, 054908 (2012).
[91] J. Adams *et al.* (STAR Collaboration), Phys. Rev. C **72**, 014904 (2005).
[92] J. W. Harris (STAR Collaboration), Nucl. Phys. **A566**, 277C (1994).
[93] M. Anderson *et al.*, Nucl. Instrum. Methods Phys. Res., Sect. A **499**, 659 (2003).
[94] B. Abelev *et al.* (STAR Collaboration), Phys. Rev. C **81**, 024911 (2010).
[95] H. Wieman *et al.* (STAR Collaboration), IEEE Trans. Nucl. Sci. **44**, 671 (1997).
[96] W. J. Llope *et al.*, Nucl. Instrum. Methods Phys. Res., Sect. A **522**, 252 (2004).
[97] A. Bilandzic, R. Snellings, and S. Voloshin, Phys. Rev. C **83**, 044913 (2011).
[98] N. Borghini, P. M. Dinh, and J.-Y. Ollitrault, Phys. Rev. C **64**, 054901 (2001).
[99] Y. Zhou, X. Zhu, P. Li, and H. Song, Phys. Rev. C **91**, 064908 (2015).
[100] N. Magdy, O. Evdokimov, and R. A. Lacey, J. Phys. G **48**, 025101 (2021).
[101] S. A. Voloshin, A. M. Poskanzer, and R. Snellings, Physics, Landolt-Bornstein **23**, 293 (2010).
[102] R. S. Bhalerao, M. Luzum, and J.-Y. Ollitrault, Phys. Rev. C **84**, 034910 (2011).
[103] G. Giacalone, J. Noronha-Hostler, and J.-Y. Ollitrault, Phys. Rev. C **95**, 054910 (2017).
[104] G. Aad *et al.* (ATLAS Collaboration), Phys. Rev. Lett. **110**, 182302 (2013).
[105] J. Adams *et al.* (STAR Collaboration), Phys. Rev. C **72**, 014904 (2005).
[106] R. A. Lacey (STAR Collaboration), Nucl. Phys. **A1005**, 122041 (2021).
[107] L. Adamczyk *et al.* (STAR Collaboration), Phys. Lett. B **743**, 333 (2015).
[108] L. Adamczyk *et al.* (STAR Collaboration), Phys. Rev. Lett. **121**, 032301 (2018).
[109] L. Adamczyk *et al.* (STAR Collaboration), Phys. Rev. C **88**, 014902 (2013).
[110] G. Agakishiev *et al.* (STAR Collaboration), Phys. Rev. C **86**, 014904 (2012).
[111] B. Schenke, C. Shen, and P. Tribedy, Phys. Rev. C **102**, 044905 (2020).
[112] B. Schenke, S. Jeon, and C. Gale, Phys. Rev. C **82**, 014903 (2010).
[113] B. Schenke, P. Tribedy, and R. Venugopalan, Phys. Rev. Lett. **108**, 252301 (2012).
[114] S. A. Bass *et al.*, Prog. Part. Nucl. Phys. **41**, 255 (1998).
[115] M. Bleicher *et al.*, J. Phys. G **25**, 1859 (1999).

[116] J. S. Moreland, J. E. Bernhard, and S. A. Bass, Phys. Rev. C **92**, 011901(R) (2015).
[117] M. Martinez, M. D. Sievert, D. E. Wertepny, and J. Noronha-Hostler, arXiv:1911.10272.
[118] A. Tumasyan *et al.* (CMS Collaboration), Phys. Rev. Lett. **129**, 022001 (2022).
[119] T. Hirano, U. W. Heinz, D. Kharzeev, R. Lacey, and Y. Nara, Phys. Rev. C **77**, 044909 (2008).
[120] S. Acharya *et al.* (ALICE Collaboration), J. High Energy Phys. 07 (2018) 103.
[121] B. Schenke, P. Tribedy, and R. Venugopalan, Phys. Rev. C **89**, 064908 (2014).